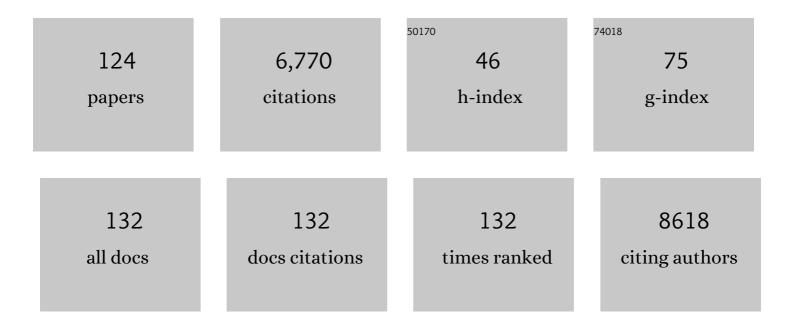
Oscar Llorca

List of Publications by Year in descending order

Source: https://exaly.com/author-pdf/337365/publications.pdf Version: 2024-02-01



OSCAP LIOPCA

#	Article	IF	CITATIONS
1	Characterization of SMG-9, an essential component of the nonsense-mediated mRNA decay SMG1C complex. Nucleic Acids Research, 2011, 39, 347-358.	6.5	384
2	Eukaryotic type II chaperonin CCT interacts with actin through specific subunits. Nature, 1999, 402, 693-696.	13.7	247
3	Three-Dimensional Structure of the Human DNA-PKcs/Ku70/Ku80 Complex Assembled on DNA and Its Implications for DNA DSB Repair. Molecular Cell, 2006, 22, 511-519.	4.5	223
4	Structure of the Hsp110:Hsc70 Nucleotide Exchange Machine. Molecular Cell, 2008, 31, 232-243.	4.5	202
5	Human C3 mutation reveals a mechanism of dense deposit disease pathogenesis and provides insights into complement activation and regulation. Journal of Clinical Investigation, 2010, 120, 3702-3712.	3.9	195
6	Eukaryotic chaperonin CCT stabilizes actin and tubulin folding intermediates in open quasi-native conformations. EMBO Journal, 2000, 19, 5971-5979.	3.5	193
7	C3 glomerulopathy–associated CFHR1 mutation alters FHR oligomerization and complement regulation. Journal of Clinical Investigation, 2013, 123, 2434-2446.	3.9	176
8	Assembly and Regulation of the Membrane Attack Complex Based on Structures of C5b6 and sC5b9. Cell Reports, 2012, 1, 200-207.	2.9	161
9	Structure of Epac2 in complex with a cyclic AMP analogue and RAP1B. Nature, 2008, 455, 124-127.	13.7	155
10	The Antibacterial Cell Division Inhibitor PC190723 Is an FtsZ Polymer-stabilizing Agent That Induces Filament Assembly and Condensation. Journal of Biological Chemistry, 2010, 285, 14239-14246.	1.6	152
11	The 'sequential allosteric ring' mechanism in the eukaryotic chaperonin-assisted folding of actin and tubulin. EMBO Journal, 2001, 20, 4065-4075.	3.5	130
12	3D architecture of DNA Pol Î \pm reveals the functional core of multi-subunit replicative polymerases. EMBO Journal, 2009, 28, 1978-1987.	3.5	112
13	Structural model of fullâ€length human Ku70–Ku80 heterodimer and its recognition of DNA and DNAâ€PKcs. EMBO Reports, 2007, 8, 56-62.	2.0	111
14	Structural and Functional Studies of LRP6 Ectodomain Reveal a Platform for Wnt Signaling. Developmental Cell, 2011, 21, 848-861.	3.1	109
15	3D reconstruction of the ATP-bound form of CCT reveals the asymmetric folding conformation of a type II chaperonin. Nature Structural Biology, 1999, 6, 639-642.	9.7	102
16	Energetics and Geometry of FtsZ Polymers: Nucleated Self-Assembly of Single Protofilaments. Biophysical Journal, 2008, 94, 1796-1806.	0.2	100
17	Three-Dimensional Structure and Regulation of the DNA-Dependent Protein Kinase Catalytic Subunit (DNA-PKcs). Structure, 2005, 13, 243-255.	1.6	98
18	Iterative Elastic 3D-to-2D Alignment Method Using Normal Modes for Studying Structural Dynamics of Large Macromolecular Complexes. Structure, 2014, 22, 496-506.	1.6	90

#	Article	IF	CITATIONS
19	Architecture of the mycobacterial type VII secretion system. Nature, 2019, 576, 321-325.	13.7	89
20	Structural Model of Human Endoglin, a Transmembrane Receptor Responsible for Hereditary Hemorrhagic Telangiectasia. Journal of Molecular Biology, 2007, 365, 694-705.	2.0	88
21	The formation of symmetrical GroEL-GroES complexes in the presence of ATP. FEBS Letters, 1994, 345, 181-186.	1.3	86
22	Structural basis for the stabilization of the complement alternative pathway C3 convertase by properdin. Proceedings of the National Academy of Sciences of the United States of America, 2013, 110, 13504-13509.	3.3	86
23	Threeâ€dimensional reconstruction of a recombinant influenza virus ribonucleoprotein particle. EMBO Reports, 2001, 2, 313-317.	2.0	85
24	Structural Model for the Mannose Receptor Family Uncovered by Electron Microscopy of Endo180 and the Mannose Receptor. Journal of Biological Chemistry, 2006, 281, 8780-8787.	1.6	76
25	3D structure of the C3bB complex provides insights into the activation and regulation of the complement alternative pathway convertase. Proceedings of the National Academy of Sciences of the United States of America, 2009, 106, 882-887.	3.3	76
26	Structures of SMG1-UPFs Complexes: SMG1 Contributes to Regulate UPF2-Dependent Activation of UPF1 in NMD. Structure, 2014, 22, 1105-1119.	1.6	74
27	Flexible tethering of primase and DNA Pol \hat{I}_{\pm} in the eukaryotic primosome. Nucleic Acids Research, 2011, 39, 8187-8199.	6.5	72
28	The nonsense-mediated mRNA decay SMG-1 kinase is regulated by large-scale conformational changes controlled by SMG-8. Genes and Development, 2011, 25, 153-164.	2.7	72
29	Three-dimensional model for the isolated recombinant influenza virus polymerase heterotrimer. Nucleic Acids Research, 2007, 35, 3774-3783.	6.5	71
30	Topology of the components of the DNA packaging machinery in the phage φ29 prohead. Journal of Molecular Biology, 2000, 298, 807-815.	2.0	70
31	Analysis of the Interaction between the Eukaryotic Chaperonin CCT and Its Substrates Actin and Tubulin. Journal of Structural Biology, 2001, 135, 205-218.	1.3	70
32	Structure of TOR and Its Complex with KOG1. Molecular Cell, 2007, 27, 509-516.	4.5	69
33	The cryo-EM structure of the UPF–EJC complex shows UPF1 poised toward the RNA 3′ end. Nature Structural and Molecular Biology, 2012, 19, 498-505.	3.6	68
34	Visualization of DNA-induced conformational changes in the DNA repair kinase DNA-PKcs. EMBO Journal, 2003, 22, 5875-5882.	3.5	67
35	Extended and bent conformations of the mannose receptor family. Cellular and Molecular Life Sciences, 2008, 65, 1302-1310.	2.4	63
36	Architecture of the Pontin/Reptin Complex, Essential in the Assembly of Several Macromolecular Complexes. Structure, 2008, 16, 1511-1520.	1.6	63

#	Article	IF	CITATIONS
37	Structural Analysis of Tobacco Etch Potyvirus HC-Pro Oligomers Involved in Aphid Transmission. Journal of Virology, 2005, 79, 3758-3765.	1.5	61
38	The three-dimensional structure of an eukaryotic glutamine synthetase: Functional implications of its oligomeric structure. Journal of Structural Biology, 2006, 156, 469-479.	1.3	61
39	Caveolar domain organization and trafficking is regulated by Abl kinases and mDia1. Journal of Cell Science, 2012, 125, 3097-113.	1.2	57
40	ATP Binding Induces Large Conformational Changes in the Apical and Equatorial Domains of the Eukaryotic Chaperonin Containing TCP-1 Complex. Journal of Biological Chemistry, 1998, 273, 10091-10094.	1.6	54
41	RPAP3 provides a flexible scaffold for coupling HSP90 to the human R2TP co-chaperone complex. Nature Communications, 2018, 9, 1501.	5.8	54
42	Recurrent Germline DLST Mutations in Individuals with Multiple Pheochromocytomas and Paragangliomas. American Journal of Human Genetics, 2019, 104, 651-664.	2.6	51
43	Human nonsense-mediated mRNA decay factor UPF2 interacts directly with eRF3 and the SURF complex. Nucleic Acids Research, 2016, 44, 1909-1923.	6.5	50
44	GroEL under Heat-Shock. Journal of Biological Chemistry, 1998, 273, 32587-32594.	1.6	49
45	Unique structure of iC3b resolved at a resolution of 24 Ã by 3D-electron microscopy. Proceedings of the United States of America, 2011, 108, 13236-13240.	3.3	49
46	Electron microscopy and 3D reconstructions reveal that human ATM kinase uses an arm-like domain to clamp around double-stranded DNA. Oncogene, 2003, 22, 3867-3874.	2.6	48
47	A Physicochemical Characterization of the Interaction between DC-Chol/DOPE Cationic Liposomes and DNA. Journal of Physical Chemistry B, 2008, 112, 12555-12565.	1.2	48
48	The Structure of the R2TP Complex Defines a Platform for Recruiting Diverse Client Proteins to the HSP90 Molecular Chaperone System. Structure, 2017, 25, 1145-1152.e4.	1.6	48
49	Conformational transitions regulate the exposure of a DNA-binding domain in the RuvBL1–RuvBL2 complex. Nucleic Acids Research, 2012, 40, 11086-11099.	6.5	47
50	The molecular and structural bases for the association of complement C3 mutations with atypical hemolytic uremic syndrome. Molecular Immunology, 2015, 66, 263-273.	1.0	47
51	Structural basis of Focal Adhesion Kinase activation on lipid membranes. EMBO Journal, 2020, 39, e104743.	3.5	47
52	HYDROMIC: prediction of hydrodynamic properties of rigid macromolecular structures obtained from electron microscopy images. European Biophysics Journal, 2001, 30, 457-462.	1.2	45
53	Compaction Process of Calf Thymus DNA by Mixed Cationicâ^'Zwitterionic Liposomes:  A Physicochemical Study. Journal of Physical Chemistry B, 2008, 112, 2187-2197.	1.2	45
54	Plasmid replication initiator RepB forms a hexamer reminiscent of ring helicases and has mobile nuclease domains. EMBO Journal, 2009, 28, 1666-1678.	3.5	45

#	Article	IF	CITATIONS
55	Type VII secretion systems: structure, functions and transport models. Nature Reviews Microbiology, 2021, 19, 567-584.	13.6	44
56	Structural comparison of prokaryotic and eukaryotic chaperonins. Micron, 2001, 32, 43-50.	1.1	43
57	A Theoretical and Experimental Approach to the Compaction Process of DNA by Dioctadecyldimethylammonium Bromide/Zwitterionic Mixed Liposomes. Journal of Physical Chemistry B, 2009, 113, 15648-15661.	1.2	42
58	Global conformational rearrangements during the activation of the GDP/GTP exchange factor Vav3. EMBO Journal, 2005, 24, 1330-1340.	3.5	41
59	The C-Terminal SH3 Domain Contributes to the Intramolecular Inhibition of Vav Family Proteins. Science Signaling, 2014, 7, ra35.	1.6	41
60	Biochemical Characterization of Symmetric GroEL-GroES Complexes. Journal of Biological Chemistry, 1996, 271, 68-76.	1.6	40
61	Structural and Functional Characterization of an Influenza Virus RNA Polymerase-Genomic RNA Complex. Journal of Virology, 2010, 84, 10477-10487.	1.5	39
62	Cyclopentenone Prostaglandins with Dienone Structure Promote Cross-Linking of the Chemoresistance-Inducing Enzyme Glutathione Transferase P1-1. Molecular Pharmacology, 2010, 78, 723-733.	1.0	39
63	The RNA helicase DHX34 functions as a scaffold for SMG1-mediated UPF1 phosphorylation. Nature Communications, 2016, 7, 10585.	5.8	39
64	Conformational Changes in the GroEL Oligomer during the Functional Cycle. Journal of Structural Biology, 1997, 118, 31-42.	1.3	38
65	Excluded Volume Effects on the Refolding and Assembly of an Oligomeric Protein. Journal of Biological Chemistry, 2001, 276, 957-964.	1.6	38
66	The AAA+ proteins Pontin and Reptin enter adult age: from understanding their basic biology to the identification of selective inhibitors. Frontiers in Molecular Biosciences, 2015, 2, 17.	1.6	37
67	Structure of Yin Yang 1 Oligomers That Cooperate with RuvBL1-RuvBL2 ATPases. Journal of Biological Chemistry, 2014, 289, 22614-22629.	1.6	36
68	Point Mutations in a Hinge Linking the Small and Large Domains of β-Actin Result in Trapped Folding Intermediates Bound to Cytosolic Chaperonin CCT. Journal of Structural Biology, 2001, 135, 198-204.	1.3	35
69	Coexistence of Closed and Open Conformations of Complement Factor B in the Alternative Pathway C3bB(Mg2+) Proconvertase. Journal of Immunology, 2009, 183, 7347-7351.	0.4	35
70	Self-Organization of FtsZ Polymers in Solution Reveals Spacer Role of the Disordered C-Terminal Tail. Biophysical Journal, 2017, 113, 1831-1844.	0.2	35
71	Assembly of the asymmetric human \hat{l}^3 -tubulin ring complex by RUVBL1-RUVBL2 AAA ATPase. Science Advances, 2020, 6, .	4.7	34
72	Symmetric GroEL-GroES complexes can contain substrate simultaneously in both GroEL rings. FEBS Letters, 1997, 405, 195-199.	1.3	33

#	Article	IF	CITATIONS
73	Biochemical Characterization of the Transcriptional Regulator BzdR from Azoarcus sp. CIB. Journal of Biological Chemistry, 2010, 285, 35694-35705.	1.6	33
74	Lessons from functional and structural analyses of disease-associated genetic variants in the complement alternative pathway. Biochimica Et Biophysica Acta - Molecular Basis of Disease, 2011, 1812, 12-22.	1.8	33
75	Structural mechanism for regulation of the AAA-ATPases RUVBL1-RUVBL2 in the R2TP co-chaperone revealed by cryo-EM. Science Advances, 2019, 5, eaaw1616.	4.7	33
76	Partial Occlusion of Both Cavities of the Eukaryotic Chaperonin with Antibody Has No Effect upon the Rates of β-Actin or α-Tubulin Folding. Journal of Biological Chemistry, 2000, 275, 4587-4591.	1.6	31
77	Gene vectors based on DOEPC/DOPE mixed cationic liposomes: a physicochemical study. Soft Matter, 2011, 7, 5991.	1.2	31
78	Addition of electrophilic lipids to actin alters filament structure. Biochemical and Biophysical Research Communications, 2006, 349, 1387-1393.	1.0	30
79	Structure of Human Complement C8, a Precursor to Membrane Attack. Journal of Molecular Biology, 2011, 405, 325-330.	2.0	30
80	Long Noncoding RNA NIHCOLE Promotes Ligation Efficiency of DNA Double-Strand Breaks in Hepatocellular Carcinoma. Cancer Research, 2021, 81, 4910-4925.	0.4	30
81	Electrochemical, Microscopic, and Spectroscopic Characterization of Prevesicle Nanostructures and Vesicles on Mixed Cationic Surfactant Systems. Langmuir, 2006, 22, 4027-4036.	1.6	29
82	A Humanized Antibody That Regulates the Alternative Pathway Convertase: Potential for Therapy of Renal Disease Associated with Nephritic Factors. Journal of Immunology, 2014, 192, 4844-4851.	0.4	29
83	RUVBL1–RUVBL2 AAA-ATPase: a versatile scaffold for multiple complexes and functions. Current Opinion in Structural Biology, 2021, 67, 78-85.	2.6	29
84	Threeâ€dimensional interplay among the ligandâ€binding domains of the urokinaseâ€plasminogenâ€activatorâ€receptorâ€associated protein, Endo180. EMBO Reports, 2003, 4, 807-812.	2.0	28
85	Molecular Architecture and Structural Transitions of a Clostridium thermocellum Mini-Cellulosome. Journal of Molecular Biology, 2011, 407, 571-580.	2.0	28
86	pH-controlled quaternary states of hexameric DnaB helicase. Journal of Molecular Biology, 2000, 303, 383-393.	2.0	27
87	Amyloidogenesis of Bacterial Prionoid RepA-WH1 Recapitulates Dimer to Monomer Transitions of RepA in DNA Replication Initiation. Structure, 2015, 23, 183-189.	1.6	26
88	The structures of cytosolic and plastid-located glutamine synthetases from <i>Medicago truncatula</i> reveal a common and dynamic architecture. Acta Crystallographica Section D: Biological Crystallography, 2014, 70, 981-993.	2.5	25
89	Conformational Changes Generated in GroEL during ATP Hydrolysis as Seen by Time-resolved Infrared Spectroscopy. Journal of Biological Chemistry, 1999, 274, 5508-5513.	1.6	24
90	Electron microscopy of Xrcc4 and the DNA ligase IV–Xrcc4 DNA repair complex. DNA Repair, 2009, 8, 1380-1389.	1.3	24

#	Article	IF	CITATIONS
91	Structural insights on complement activation. FEBS Journal, 2015, 282, 3883-3891.	2.2	22
92	3D structure of Syk kinase determined by single-particle electron microscopy. Biochimica Et Biophysica Acta - Proteins and Proteomics, 2007, 1774, 1493-1499.	1.1	21
93	Effects of the Inter-ring Communication in GroEL Structural and Functional Asymmetry. Journal of Biological Chemistry, 1997, 272, 32925-32932.	1.6	20
94	Evidence for a remodelling of DNA-PK upon autophosphorylation from electron microscopy studies. Nucleic Acids Research, 2011, 39, 5757-5767.	6.5	20
95	Modulation of the Chaperone DnaK Allosterism by the Nucleotide Exchange Factor GrpE. Journal of Biological Chemistry, 2015, 290, 10083-10092.	1.6	20
96	Structure of the TELO2-TTI1-TTI2 complex and its function in TOR recruitment to the R2TP chaperone. Cell Reports, 2021, 36, 109317.	2.9	20
97	Conformational rearrangements upon Syk auto-phosphorylation. Biochimica Et Biophysica Acta - Proteins and Proteomics, 2009, 1794, 1211-1217.	1.1	19
98	Aggregation Phenomena on the Ternary Ionicâ^'Nonionic Surfactant System: Didodecyldimethylammonium Bromide/Octyl-β-d-glucopyranoside/Water. Mixed Microaggregates, Vesicles, and Micelles. Langmuir, 2005, 21, 1795-1801.	1.6	18
99	Reconstitution of the Escherichia coli cell division ZipA–FtsZ complexes in nanodiscs as revealed by electron microscopy. Journal of Structural Biology, 2012, 180, 531-538.	1.3	18
100	Introduction to 3D reconstruction of macromolecules using single particle electron microscopy1. Acta Pharmacologica Sinica, 2005, 26, 1153-1164.	2.8	15
101	Advances on the Structure of the R2TP/Prefoldin-like Complex. Advances in Experimental Medicine and Biology, 2018, 1106, 73-83.	0.8	15
102	Prediction of the structure of GroES and its interaction with GroEL. Proteins: Structure, Function and Bioinformatics, 1995, 22, 199-209.	1.5	14
103	Electron microscopy studies on DNA recognition by DNA-PK. Micron, 2004, 35, 625-633.	1.1	14
104	A Novel Antibody against Human Factor B that Blocks Formation of the C3bB Proconvertase and Inhibits Complement Activation in Disease Models. Journal of Immunology, 2014, 193, 5567-5575.	0.4	14
105	Structural basis for substrate specificity of heteromeric transporters of neutral amino acids. Proceedings of the National Academy of Sciences of the United States of America, 2021, 118, .	3.3	11
106	ATP hydrolysis induces an intermediate conformational state in GroEL. FEBS Journal, 1999, 259, 347-355.	0.2	10
107	Caveolar domain organization and trafficking is regulated by Abl kinases and mDia1. Journal of Cell Science, 2012, 125, 4413-4413.	1.2	10
108	RPAP3 C-Terminal Domain: A Conserved Domain for the Assembly of R2TP Co-Chaperone Complexes. Cells, 2020, 9, 1139.	1.8	10

#	Article	IF	CITATIONS
109	Structure and Assembly of the PI3K-like Protein Kinases (PIKKs) Revealed by Electron Microscopy. AIMS Biophysics, 2015, 2, 36-57.	0.3	10
110	Electron microscopy reconstructions of DNA repair complexes. Current Opinion in Structural Biology, 2007, 17, 215-220.	2.6	9
111	Regulation of RUVBL1-RUVBL2 AAA-ATPases by the nonsense-mediated mRNA decay factor DHX34, as evidenced by Cryo-EM. ELife, 2020, 9, .	2.8	9
112	Role of the amino terminal domain in GroES oligomerization. BBA - Proteins and Proteomics, 1997, 1337, 47-56.	2.1	6
113	Cationic Prevesicle and Vesicle Nanoaggregates:Â An Experimental and Theoretical Study. Journal of Physical Chemistry B, 2006, 110, 23524-23539.	1.2	6
114	How novel structures inform understanding of complement function. Seminars in Immunopathology, 2018, 40, 3-14.	2.8	6
115	CryoEM of RUVBL1–RUVBL2–ZNHIT2, a complex that interacts with pre-mRNA-processing-splicing factor 8. Nucleic Acids Research, 2022, 50, 1128-1146.	6.5	6
116	Functional and structural characterization of four mouse monoclonal antibodies to complement C3 with potential therapeutic and diagnostic applications. European Journal of Immunology, 2017, 47, 504-515.	1.6	5
117	Ionic tethering contributes to the conformational stability and function of complement C3b. Molecular Immunology, 2017, 85, 137-147.	1.0	5
118	Structural insights into nonsense-mediated mRNA decay (NMD) by electron microscopy. Current Opinion in Structural Biology, 2013, 23, 161-167.	2.6	4
119	TubZ filament assembly dynamics requires the flexible C-terminal tail. Scientific Reports, 2017, 7, 43342.	1.6	3
120	Modeling of a 14 kDa RUVBL2-Binding Domain with Medium Resolution Cryo-EM Density. Journal of Chemical Information and Modeling, 2020, 60, 2541-2551.	2.5	3
121	Three-Dimensional Structure and Regulation of the DNA-Dependent Protein Kinase Catalytic Subunit (DNA-PKcs). Structure, 2005, 13, 495.	1.6	1
122	Electron microscopy reveals coexistence of distinct conformations of iC3b. Immunobiology, 2012, 217, 1166.	0.8	0
123	Flexible tethering of primase and DNA Pol in the eukaryotic primosome. Nucleic Acids Research, 2012, 40, 4726-4726.	6.5	0
124	Structure of the TELO2-TTI1-TTI2 Complex and its Function in TOR Recruitment to the R2TP Chaperone. SSRN Electronic Journal, 0, , .	0.4	0